Engineering and Technology Journal
Journal homepage: https://etj.uotechnology.edu.iq

Properties of Welded Copper Tubes Fabricated Via Friction crush Welding

Abdul Jabbar S. Jomah[a*], **Akeel D. Subhi**[b], **Fadhil A. Hashim**[c]

[a] Materials Engineering Dept, College of Engineering, University of Diyala, Diyala, Iraq
[b] Production Engineering and Metallurgy Dept, University of Technology-Iraq, Alsina'a Street, 10066 Baghdad, Iraq.
[c] Materials Engineering Dept, University of Technology-Iraq, Alsina'a Street, 10066 Baghdad, Iraq.
*Corresponding author Email: mailto:abdaljabar.saad@uodiyala.edu.iq

HIGHLIGHTS

- Characterization and evaluation of mechanical properties of welded tubes made from oxygen-free copper (C1020) sheet using friction crush welding were investigated.
- The microstructure study showed good weld quality and good material flow between the two ends of the copper sheet in the weld zone.
- The results also showed that ductile fracture is the main source of failure.

ABSTRACT

The welding process is one of the fabrication processes in which tubes can be performed for structural purposes and transport liquids or gases. This study is focused on the manufacturing, characterization, and evaluation of mechanical properties of welded tubes made from oxygen-free copper (C1020) sheets using friction crush welding. The welded tubes were produced using different tool rotation speeds (1500, 1600, and 1700 rpm) and feed rates (130, 140, and 150 mm/min). The flanged edge height of 2.5 mm and 0.5 mm gap between the ends of the copper sheet was used. All examinations on welded tubes were achieved using different instruments such as optical microscopy, SEM, hardness, and tensile testers. The microstructure study showed good weld quality and good material flow between the two ends of the copper sheet in the weld zone. Moreover, the weld zone was not defective. The lowest hardness was identified in the crush zone due to the coarseness of the copper grains. The highest tensile strength of 105 MPa was obtained at the tool rotation speed of 1500 rpm and 130 mm/min feed rate. The results also showed that ductile fracture is the main source of failure.

ARTICLE INFO

Handling editor: Israa A. Aziz

Keywords: Welded tubes; copper tube; friction crush welding, solid-state welding; friction welding.

1. Introduction

Industrial friction welding applications have increased in recent years, such as in electronic packages, engines, fuel tanks, tubes, pipelines, and many other applications [1,3]. Friction welding is used for joining materials in a solid-state where the produced heat is due to a relative movement between two components under pressure. Conventional friction welding processes such as rotary, linear, and orbital friction welding are categorized according to the nature of the movement relative to their interfaces and in accordance with their type of energy supply. The weld zone has a characteristically fine-grained microstructure, and the joint shows a narrow heat-affected zone [4]. Therefore, a non-consumable welding tool provides the required temperature and plastic deformation over the welding area [5]. Friction crush welding (FCW) is one of the welding techniques used to weld thin sheets [6]. The concept of the FCW process is simple where a non-consumable rotating tool with a specific disk geometry and profile is used for crushing a certain volume of base metal [7,8]. It is based on the friction caused by the relative motion between the non-consumable rotating tool and the workpiece surface. A uniform unidirectional relative velocity is used to weld similar and dissimilar sheet metals [9,10].

Generally, tubes or pipes are made on a large scale using several welding processes such as electric resistance welding, electric arc welding, high-frequency welding, and submerged arc welding [11,12,13,14]. Machining operations are needed to remove the internal and external flash defects. External flash is easy to remove by machining processes, but internal flash is hardly removed [15]. In addition, conventional friction welding is not compatible with thin-walled pipes. By controlling the relative motion of the tool, friction stir welding (FSW) can be used to join thin-walled pipes to avoid defects encountered in

http://doi.org/10.30684/etj.v40i6.2292
Received 24 July 2021; Accepted 06 September 2021; Available online 09 May 2022
2412-0758/University of Technology-Iraq, Baghdad, Iraq

conventional welding processes [16]. Previous investigations have referred to pip-pipe welding using friction welding techniques [17,18,19], and few types of research have been done on FCW [20,21]. Still, no one has mentioned the fabrication of pipes from C1020 copper sheets or other materials using FCW. This study is a relatively new investigation investigating the fabrication and characterization of welded tubes made from C1020 copper sheets without internal flash using FCW with different processing parameters. Exuded water and pressurized air tests were also performed to determine the ability of welded tubes to transport liquid and gaseous media.

2. Experimental work

2.1 Material and Experimental Setup

Oxygen-free copper (C1020) sheet with dimensions of (100 mm x 60 mm x 1mm) was used to fabricate welded tubes. The chemical composition of the oxygen-free copper (C1020) sheet is illustrated in Table 1. Several welded tubes were fabricated using different FCW parameters, and all of them were evaluated using microstructural characterization and mechanical properties investigation. The mechanical properties of the copper (C1020) sheet are given in Table 2. The hardness of the FCWed copper (C1020) joint was measured by the Vickers hardness tester model (HVS-1000). A 500 g load was applied during the hardness test on the cross-section of the welded joint for 15 s. Figure 1 shows the FCW process achieved using a universal horizontal milling machine type (IWASHITA, Japan) with a motor power of 5 KW. The FCW tool was rotated at different speeds such as1500, 1600, and 1700 rpm. On the other hand, the different linear speeds used in the experiments were 130, 140, and 150 mm/min. The flanged edge height of 2.5 mm and gap of 0.5mm between the ends of the copper sheet was used in all experiments.

2.2 Crushing material and manufacturing of tool

Figure 2 shows the schematic diagram of the joint design at the two ends of the copper sheet with a flanged edge to fabricate the welded tube. The height of the flanged edge depended on the total sum of gap volume and profile volume [7]. The general rule for determining the volume was based on the total volume before deformation equal to the total volume after deformation. The formulas used for the calculation of flanged edge height (A), the total height of flange (F), and total volume are described elsewhere [9]. The FCW tool used in all experiments was manufactured from high-strength low alloy steel (A514 R) with chemical composition illustrated in Table 3. Some of the welded copper tubes, the support tools needed in the fabrication of the welded tubes, and the FCW tool and its dimensions are shown in Figure 3.

The tensile test specimens have been prepared according to DIN EN ISO 4136 standard. Tensile test was performed using universal testing machine model WDW-200E. Microstructural investigation of the weld zone was conducted by preparing the cross-section of the welded joint surface using grinding, polishing, and etching, respectively. The etching was achieved using (5 g $FeCl_3$, 50 ml HCl, and 100 ml distilled water) etching solution. Optical microscope type Optika-Italy and scanning electron microscopy (SEM) type (FEI 9922650) with high-resolution were used to characterize the microstructure.

Table 1: Chemical composition of oxygen-free copper (C1020) sheet

Element wt.%	Si	Fe	Sn	Mn	Ni	Zn	Ag	Pb	Bi	Cu
Measured	0.004	0.003	0.002	0.003	0.005	0.02	0.002	0.010	0.005	Balance

Table 2: Mechanical properties of Oxygen-free copper (C1020) sheet

Base materials	Tensile Strength MPa	Elongation %	Hardness HV
Copper (C1020)	180	15	80

Table 3: Chemical composition of friction crush welding tool (A514 R)

Element wt.%	C	Si	Mn	Ni	W	Co	Cr	Mo	V	Fe
A514 R	0.234	0.253	0.894	0.390	0.025	0.018	0.567	0.167	0.007	Balance

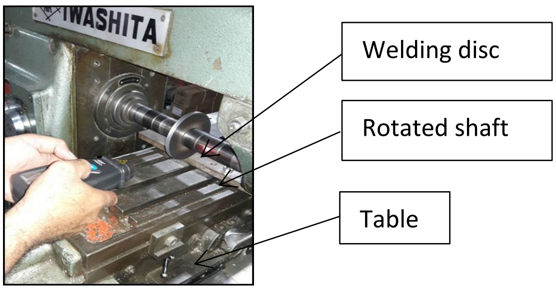

Figure 1: Horizontal milling machine used for FCW

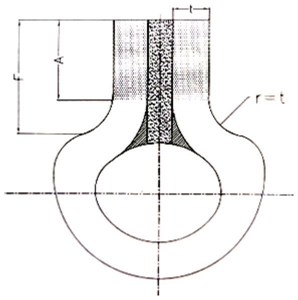

Figure 2: Schematic diagram of the joint design at the two ends of the copper sheet for tube fabrication

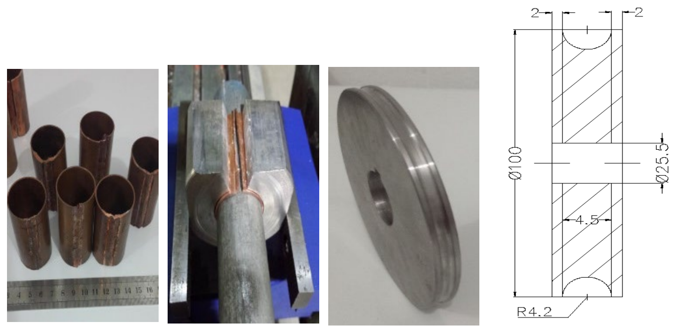

(a) (b) (c) (d)

Figure 3: a- some welded copper tubes fabricated via FCW, b- support tools needed in the manufacture of welded tube, c- FCW tool, and d- dimensions of FCW tool in mm

2.3 Fabrication of tubes by FCW process

A copper sheet with a flanged edge was wrapped around a support rod and enclosed in a support mold using special pliers. The movement of the rotated welding disc along the welding line at the flanged edge using specific rotation speeds and feed rates resulted in the welding of the tube. Several successful attempts have been made to fabricate welded tubes. The fabrication of the FCW welded tube is illustrated in Figure 4.

2.4 Examination of welded tubes

Welded copper tubes can be examined using pressurized air and exuded water tests, which can be called hydro-pneumatic testing methods, according to (ASME B31.3 and BPV section VIII) [22,23].

2.4.1 Exuded water test

In this test, the lower end of the welded tube was closed with a water plug. Then, the tube was filled with water and the water temperature during the test was (15 C°). Then, the water was left in the welded tube for a while (20 min) under atmosphere pressure to observe if there was any water leakage [22,23]. Figure 5 shows the exuded water test.

2.4.2 Pressurized air test

The welded tube was closed at both ends and compressed with air in this test. The pressure gauge was connected to the tube, and the pressurized air leakage was observed for a period (10 min) under the pressure of (0.0689 MPa) [22,23]. Figure 6 shows the pressurized air test.

3. Results and discussion

3.1 Hydro-Pneumatic Test Study

The hydro-pneumatic tests (exuded water and pressurized air tests) identified that no water or pressurized air leaked through the welding line because the weld area was defectless, and the gap between the two ends of the copper sheet was filled during the FCW. The macrograph of an FCWed copper tube joint with a tool rotation speed of 1500 rpm and a feed rate of 130 mm/min can be shown in Figure 7. The outer side of the welded tube along the welding line clearly showed some external flash which is easy to remove with the machining processes (Figure7-a). It is important to realize that no internal flash can be observed in the inside diameter of the welded tube along the welding line (Figure7-b). From this, it is important to conclude that friction crush welding was suitable for use in the tube production process

3.2 Microstructure Study

The microstructure of the welded copper tube joint at a rotational tool speed of 1500 rpm and a feed rate of 130 mm/min can be shown in Figure 8. It is evident that the distinct regions evolved during FCW, such as crush zone (CZ), thermo-mechanically affected zone (TMAZ), and heat-affected zone (HAZ). The microstructure also shows good weld quality and good material flow between the two ends of the copper sheet in the weld zone and the weld zone, which was not defective. Figure 8-a shows the microstructure of base metal (BM), observing the copper grains. At the same time, Figure 8-b shows the microstructure (HAZ), as this region was only exposed to the thermal cycle, and thus grain growth appeared. Figure 8-c shows the microstructure of TMAZ in which copper grains are subjected to both heating and plastic deformation during FCW and characterized by a deformed microstructure caused by the mechanical crushing resulting from the FCW tool. Finally, Figure 8-d represents the microstructure of the crush zone (CZ). This zone is recognized by fine and equiaxed dynamic recrystallized grains without weld defects and complete gap filling between the two ends of the copper sheet.

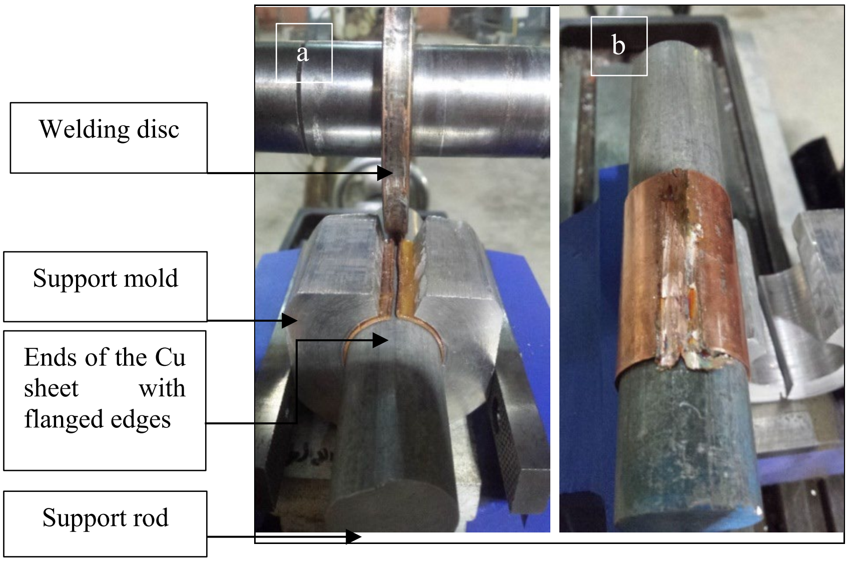

Figure 4: a- FCW used to fabricate copper tube, b- copper welded tube after fabrication

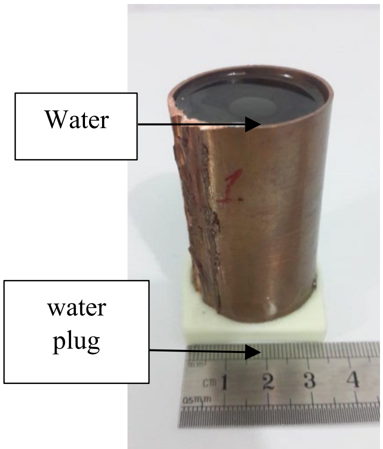

Figure 5: Exuded water test

Figure 6: pressurized air test

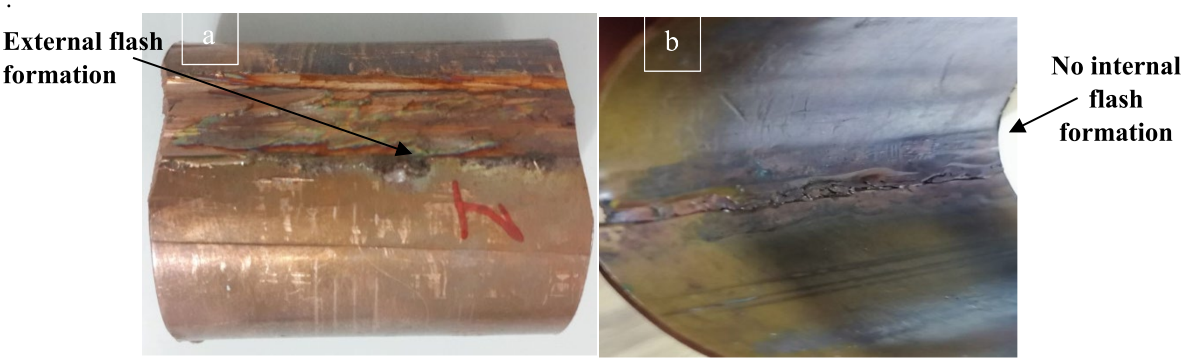

Figure 7: Macrograph of FCWed copper tube joint at rotational tool speed of 1500 rpm and

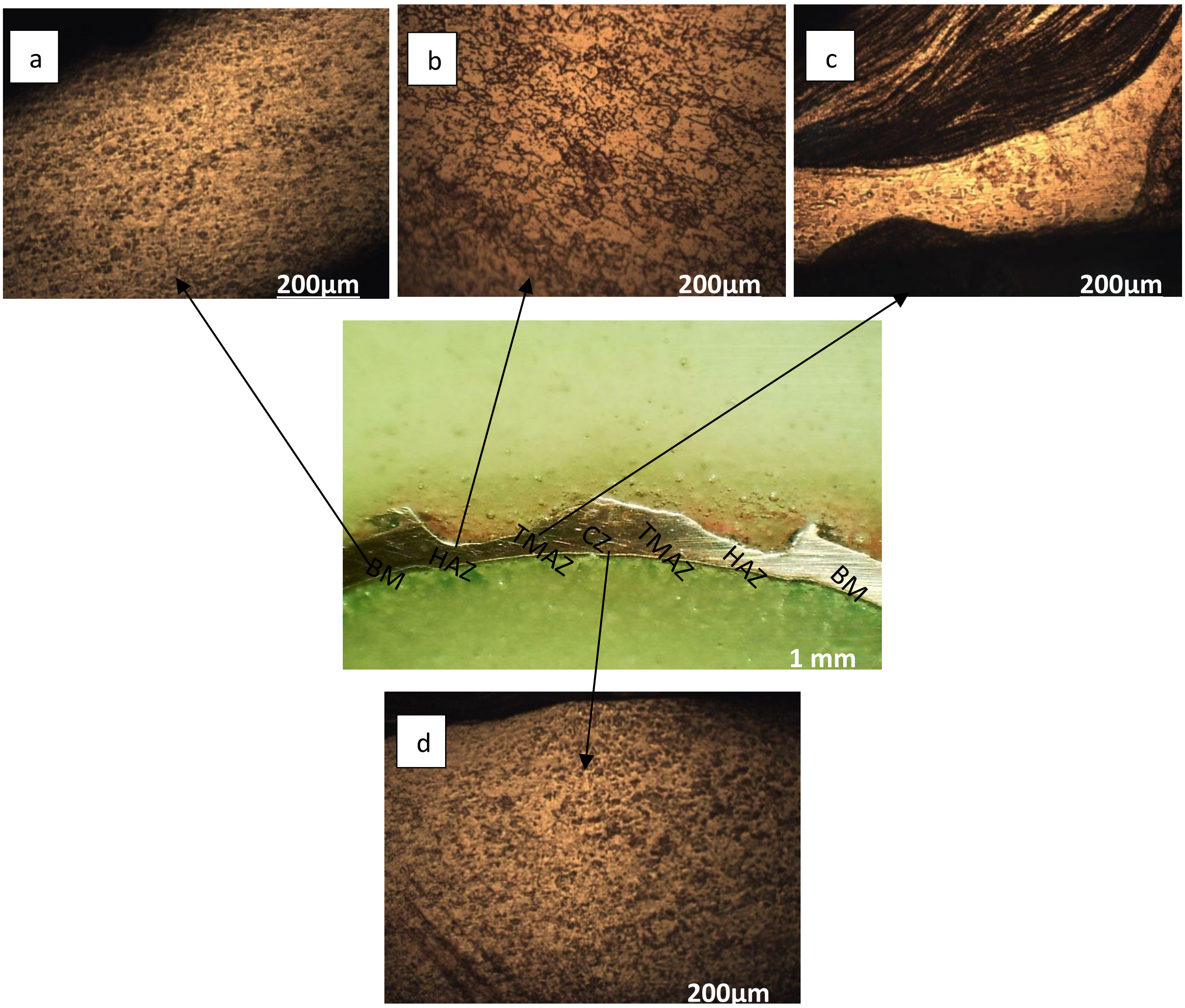

Figure 8: Cross-section microstructure of welded tube joint at rotational tool speed of 1500 rpm and feed rate of 130 mm/min, (a) base metal, (b) heat-affected zone, (c) thermo-mechanical affected zone, (d) crush zone

3.3 Hardness Evaluation

The relationship between hardness and distance along the cross-sectional area of the FCWed tube joint at different tool rotation speeds and feed rates is illustrated in Figure 9. It is clear that the weld S1 had the highest hardness of 62 HV, and the hardness values of the welds S2 to S9 were 60 HV, 58 HV, 55 HV, 53 HV, 50 HV, 49 HV, 48 HV, 45 HV, respectively. The total hardness gradually decreases from base metal to a certain value in the crush zone for each weld. Generally, the base metal has the highest hardness of approximately 80 HV, while the lowest value of 45 HV was found in the crush zone of weld S9. This indicates that the hardness distribution along the cross-section of the FCWed tube joint was affected by metallurgical changes represented by distinct regions recognized in the weld zone. Increased tool rotation speed and feed rate increased heat generation due to the higher friction between the FCW disc and the ends of the copper sheet during welding, resulting in increased grain size. The coarse grain reduced the hardness and bond strength. This reflects the decrease in the hardness value in the crush zone of all FCWed copper tube joints.

3.4 Tensile Test Study

Figure 10 shows the stress-strain curves of the C1020 sheet and FCWed copper tube joints. Oxygen-free copper sheet has the highest tensile strength of 180 MPa and elongation of 15% compared with welded copper tube joints. For FCWed tube joints, the tensile strength and elongation of specimen S9 to specimen S1 were increased. The tensile strength of specimen S1 was about 105 MPa, and this value corresponds to 60% of the strength of C1020. The elongation was 10%, as the crush zone possesses fine, equiaxed dynamic recrystallized grains without welding defects and filling the gap between the two ends of the copper sheet. The tensile strength of specimen S2 was about 65 MPa, and the elongation was 6%. This decrease in tensile strength and elongation may be related to the presence of some weld defects and an increase in the feed rate. The tensile strength of specimen S3 was about 60 MPa, and elongation was 5%, which may be due to the cracks in the crush zone and an increase in the feed rate. Whereas 57 MPa, 55 MPa, and 53 MPa of tensile strengths with 5.5%, 5%, and 4.5% of elongation were obtained for specimens S4, S5, and S6, respectively. This decrease in tensile strength and elongation may result from the crush zone having many defects like cracks. For specimens S7, S8, and S9, the tensile strength was about 49 MPa, 48 MPa, and 46 MPa, respectively, and the elongation was 4%, 3.8%, and 3.5%, respectively. Generally, the decrease in the mechanical properties may be related to the large heat input and various defects such as cracks and over-crushing due to increased tool rotational speed and feed rate.

Figure 11 shows the SEM micrographs of different locations in the crush zone of welded copper tube joints. The good quality of weld joints, good material flow between the ends of copper sheet, complete welding along the welding line, and excessive crush can be shown in Figure 11-S1. Figure 11-S2 shows the welded tube joint with a good flow of material between the ends of the copper sheet with some defects such as cracks and excessive crush due to the increase in the feed rate. This led to an increase in the heat input. Figure 11-S3 shows the quality of the welded joint, which is represented by the crush zone, decreases due to an increase in the weld defects such as cracks and excessive crush. This is because the material flow between the two ends of the copper sheet decreases with the increase in the feed rate and the decrease in heat generation.

Figure 12 shows SEM micrographs of the fracture surface of an FCWed copper tube joint at a tool rotation speed of 1500 rpm and a feed rate of 130 mm/min. The fracture surface due to the tensile test of the joint shows the presence of identifiable dimples. Each dimple on the fracture surface corresponds to avoiding. The crushed area is the weakest area of the FCWed tube joint due to it has the lowest hardness. Hence the fracture occurs in this area. The fracture surface topography indicated that the ductile fracture mechanism is the main source of fracture.

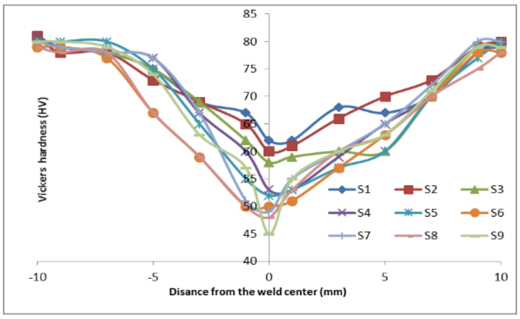

Figure 9: The hardness distribution along the cross-sectional area of FCWed copper tube joints at various tool rotation speeds and feed rates: (S1) 1500 rpm and 130 mm/min, (S2) 1500 rpm and 140 mm/min, (S3) 1500 rpm and 150 mm/min, (S4) 1600 rpm and 130 mm/min, (S5) 1600 rpm and 140 mm/min, (S6) 1600 rpm and 150 mm/min, (S7) 1700 rpm and 130 mm/min, (S8) 1700 rpm and 140 mm/min, (S9) 1700 rpm and 150 mm/min

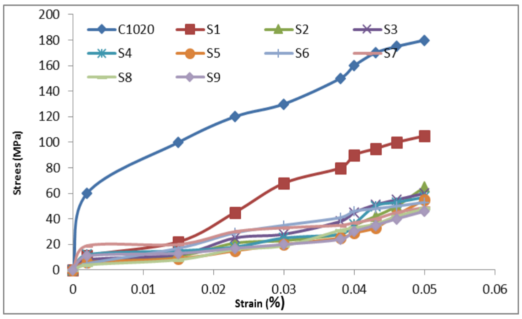

Figure 10: Stress-strain curves of the oxygen-free copper sheet and FCWed copper tube joints at various tool rotation speeds and feed rates: (S1) 1500 rpm and 130 mm/min, (S2) 1500 rpm and 140 mm/min, (S3) 1500 rpm and 150 mm/min, (S4) 1600 rpm and 130 mm/min, (S5) 1600 rpm and 140 mm/min, (S6) 1600 rpm and 150 mm/min, (S7) 1700 rpm and 130 mm/min, (S8) 1700 rpm and 140 mm/min and (S9) 1700 rpm and 150 mm/min

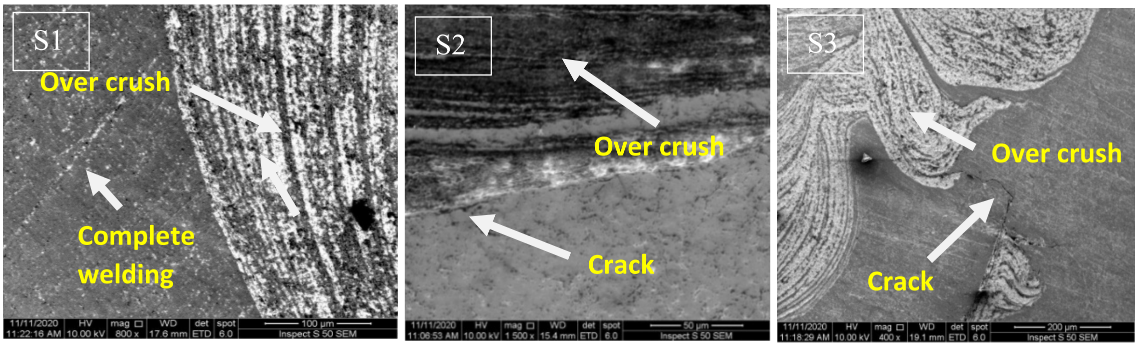

Figure 11: Scanning electron microscope images at different locations in the crush zone of welded copper tube joints using different rotational speeds and feed rates: S1- 1500 rpm and 130 mm/min, S2- 1500 rpm and 140 mm/min, S3-1500 rpm and 150 mm/min

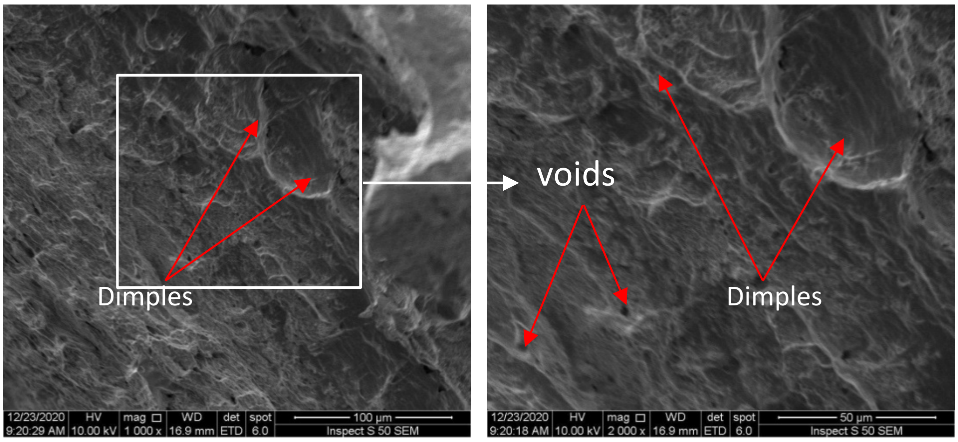

Figure 12: SEM images of the fracture surface of tensile tested welded tube at a tool rotation speed of 1500 rpm and feed rate of 130 mm/min

4. Conclusion

1. The fabrication of welded copper tube can be successfully achieved using FCW without the formation of a flash in the inside diameter of the welded tube along the welding line.
2. Microstructural observations of the FCWed copper tube joints demonstrated the good weld quality and good material flow between the two ends of the copper sheet in the weld zone. In addition, the weld zone was free from defects with complete defects gap filling between the two ends of the copper sheet.
3. The hardness and tensile strength of FCWed copper tube joints decrease with tool rotation speed and feed rate increase.
4. The highest hardness and maximum tensile strength of FCWed copper tube joints were 62 HV and 105 MPa, respectively, obtained at a tool rotation speed of 1500 rpm and 130 mm/min feed rate.
5. Observation of SEM images of the FCWed tube joint fracture surface revealed a ductile fracture mode.

Author contribution

All authors contributed equally to this work.

Funding

This research received no specific grant from any funding agency in the public, commercial, or not-for-profit sectors.

Data availability statement

The data that support the findings of this study are available on request from the corresponding author.

Conflicts of interest

The authors declare that there is no conflict of interest.

References

[1] M. Merklein, M. Johannes, M. Lechner, and A. Kuppert, A review on tailored blanks-Production, applications and evaluation, J. Mater. Process. Technol., 214 (2014) 151–164. https://doi.org/10.1016/j.jmatprotec.2013.08.015

[2] U. Köklü, Investigation into the formability of Al-1050 tailor-welded blanks with antilock braking system, Int. J. Adv. Manuf. Technol., 66 (2013) 221–229. https://doi.org/10.1007/s00170-012-4320-z

[3] Ismail, A. et al. 2018. The mapping of full weld cycle heat profile for friction stir welding pipe butt joints, In: Öchsner, A. (eds) Engineering Applications for New Materials and Technologies. Advanced Structured Materials, vol. 85, pp. 461–467. Springer, Cham. https://doi.org/10.1007/978-3-319-72697-7_38

[4] F.A. Besler, P. Schindele, R.J. Granta, M.J.R. Stegmüller, Advanced process possibilities in friction crush welding of aluminum, steel, and copper by using an additional wire, Metall. Mater. Trans. B, 48 (2017) 2930–2948. https://doi.org/10.1007/s11663-017-1108-4

[5] G.S. Brar, A.S. Jamwal, Friction Crush Welding of Aluminium Alloy 6061 T-6, Int. J. Adv. Multidiscip. Res., 2 (2017) 101 -104.

[6] A.S. Jomah, A.D. Subhi, F.A. Hashim, Microstructure and mechanical properties of friction crush welded joints of oxygen-free copper (C1020) sheets, Diyala. J. Eng. Sci., 13 (2020) 58-65. https://doi.10.24237/djes.2020.13306

[7] F. A. Besler, P. Schindele, R.J. Granta, M.J.R. Stegmüller, Friction crush welding of aluminium, copper and steel sheetmetals with flanged edges, J. Mater. Process. Technol., 234 (2016) 72 - 83. https://doi.org/10.1016/j.jmatprotec.2016.03.012

[8] A.S. Jomah, A.D. Subhi, F.A. Hashim, Effect of friction crush welding parameters on the properties of welded joints of C1020 copper sheet, IOP J. Phys. Conf. Ser., 1973,2021, 012048. https://dx.doi.org/10.1088/1742-6596/1973/1/012048

[9] G.S. Brar, M. Singh, A.S. Jamwal, Process parameter optimization of friction crush welding (FCW) of AISI 304 stainless steel, Proceedings of the ASME International Mechanical Engineering Congress and Exposition, Tampa, Florida, USA, 2, 2017. https://doi.org/10.1115/IMECE2017-71302

[10] A.S. Jomah, F.A. Hashim, A.D. Subhi, Metallurgical investigation and mechanical properties of dissimilar friction crush welded Cu-Al sheets with flanged edge. J. Phys. Conf. Ser., 1973, 2021, 012116. https://dx.doi.org/10.1088/1742-6596/1973/1/012116

[11] T. Hidaka, T. Kimura, S. Fujimori, New welding process in the manufacturing of UOE pipes. Trans. Iron Steel Inst. Jpn., 26 (1986) 387-394. https://doi.org/10.2355/isijinternational1966.26.387

[12] P. Simion, V. Dia, B. Istrate, C. Munteanu, Controlling and monitoring of welding parameters for micro-alloyed steel pipes produced by high frequency electric welding, Adv. Mater. Res., 1036 (2014) 464-469. https://doi.org/10.4028/www.scientific.net/AMR.1036.464

[13] D. Tat, T. Pasang, M. Ramezani, Gas tungsten arc welding of copper and mild steel, Int. J. Sci. Eng. Investig., 4 (2015) 32-38.

[14] H. Rampaul, Pipe Welding Procedures, 2nd Edition, Industrial Press Inc. New York, 2003.

[15] M.E. Abdullah, R.K. Abdel-Magied, M.N. Elsheikh, Experimental investigation of formability of Al-1050 tailor-welded blanks, Int. J. Adv. Manuf. Technol., 89 (2017) 791–801. https://doi.org/10.1007/s00170-016-9147-6

[16] A. Ismail, M. Awang, H. Fawad, and K. Ahmad, Friction stir welding on aluminum alloy 6063 pipe, in Proceedings of the 7th Asia Pacific IIW International Congress, Singapore. 67 (2013) 78–81.

[17] G.V. Beloshapkin, M.V. Beloshapkin, V.K. Pisarov, V.E. Stolberov, V.A. Chernov, Friction welding of pipes, Weld. Int. 21 (2007) 458–459. https://doi.org/10.1080/09507110701455673

[18] H. Vyas, K.P. Mehta, V. Badheka, B. Doshi, Pipe-to-pipe friction welding of dissimilar Al-SS joints for cryogenic applications, J. Braz. Soc. Mech. Sci. Eng., 42 (2020)96. https://doi.org/10.1007/s40430-020-2181-1

[19] R. Palanivel, R.F. Laubscher, I. Dinaharan, An investigation into the effect of friction welding parameters on tensile strength of titanium tubes by utilizing an empirical relationship, Measurement, 98 (2016) 77–91. https://doi.org/10.1016/j.measurement.2016.11.035

[20] M. E. Abdullah, H.T. Elmetwally, N.G. Yakoub, M.N. Elsheikh, A.A. Abd-Eltwab, Effect of orbital friction crush welding parameters on aluminum tubes, Int. J. Sci. Technol. Res., 9 (2020) 4483- 4486.

[21] H.T. Elmetwally, N.G. Yakoub, M.N. Elsheikh, A.A. Abd-Eltwab, M.E. Abdullah, Influence of friction crush welding tool profiles on the weldability of commercial aluminum tubes, Int. j. mech. prod. Eng., 10 (2020) 5579–5588.

[22] Copper Development Association Inc, Copper Tube Handbook, Industry Standard Guide for the Design and Installation of Copper Piping Systems, Published by Copper Development Association Inc., 260 Madison Avenue, New York, 2010.

[23] D. Sarma, Introduction to hydro testing-process piping, Digital magazine for industry and academia, ASME B31.3 and BPV Section VIII, (2020).